Isoscalar spin excitation in ^{40}Ca

M. Morlet,[1] E. Tomasi-Gustafsson,[2] A. Willis,[1] J. Van de Wiele,[1]
N. Marty,[1] C. Glashausser,[3] B. N. Johnson,[1,4] F. T. Baker,[5]
D. Beatty,[3] L. Bimbot,[1] C. Djalali,[4] G. W. R. Edwards,[3]
A. Green,[3,*] J. Guillot,[1] F. Jourdan,[1] H. Langevin-Joliot,[1]
L. Rosier,[1] and M. Y. Youn[6]

[1] *Institut de Physique Nucléaire, Orsay, Boite Postale No. 1, 91406, Orsay, France*
[2] *Laboratoire National Saturne, Centre d'Etudes Nucléaires Saclay, 91191 Gif-sur-Yvette CEDEX, France*
[3] *Rutgers University, New Brunswick, New Jersey 08903*
[4] *Department of Physics and Astronomy, University of South Carolina, Columbia, South Carolina 29208*
[5] *University of Georgia, Athens, Georgia 30602*
[6] *Dapnia-SPN, Centre d'Etudes Nucléaires Saclay, 91191 Gif-sur-Yvette CEDEX, France*

(Received 5 March 1992)

A signature S_d^y of isoscalar spin-transfer strength has been tested in the inelastic scattering of 400 MeV deuterons from ^{12}C. It was then applied to the study of ^{40}Ca over an angular range from 3° to 7° (momentum transfer range from 0.26 to 0.8 fm^{-1}) and an excitation energy range from 6.25 to 42 MeV. This is the first study of isoscalar spin strength in the continuum. Spin excitations were found in the 9 MeV region, and over a broad range in the continuum with a cluster strength around 15 MeV. The results are compared with spin-flip probability measurements in proton scattering. In contrast to the total relative spin response, which is strongly enhanced at high excitation, the isoscalar relative spin response is roughly consistent with noninteracting Fermi gas values.

PACS number(s): 25.45.De, 21.10.Hw, 27.40.+z

I. INTRODUCTION

Collective ΔS=0 (i.e., spin transfer 0) excitations have been extensively studied both theoretically and experimentally during the seventies [1]. Since 1980 Gamow-Teller, isovector spin-dipole, and isovector spin-quadrupole strengths have been localized by charge-exchange (p,n) and $(^3\mathrm{He},t)$ reactions [2–5]. Many 1^+ states have been studied both by electron [6] and proton inelastic scattering [7, 8]. Proton inelastic-scattering spin-transfer experiments have localized spin-dipole and spin-quadrupole strength [9–12] and have shown that ΔS=1 states are shifted to high energy compared to isoscalar ΔS=0 states. Inelastic proton scattering excites isovector as well as isoscalar states, while in the electromagnetic interaction the isoscalar spin force is small. In the nucleon-nucleon interaction, the isoscalar spin force is less than 1/3 of the isovector spin force [8]. Then, even if the isoscalar and isovector spin transition densities are of the same order, the isoscalar spin-flip cross sections are always much smaller than the isovector ones. Therefore very few isoscalar spin states are presently known, none of them in ^{40}Ca. The continuum spin response in the ΔT=0 channel is essentially unknown.

As deuteron inelastic scattering can excite only isoscalar transitions, it would be the simplest and best probe for such states, if a clear signature for ΔS=1 excitations could be found. In a previous work [13] the validity of such a signature was tested on different states of ^{12}C. This signature is used in the present work to detect isoscalar spin strength in ^{40}Ca. The present results are compared to the total spin strength localized by $(\vec{p},\vec{p}')$ scattering [9, 10, 14]. Measurements were performed between 3° and 7° (for a momentum transfer q between 0.26 and 0.8 fm^{-1}) and for excitation energies ranging from 6.25 to 42 MeV. Preliminary results have already been given in Ref. [15]. In Sec. II expressions for the spin observables that were derived in Ref. [13], and the microscopic description of deuteron-nucleus scattering are given. Section III contains the details of the experimental set-up and the procedure that was followed to extract the spin observables. The experimental results are given and discussed in Sec. IV; the conclusion is presented in section V.

II. SIGNATURE FOR SPIN-FLIP TRANSITIONS

In $(\vec{p},\vec{p}')$ scattering [16] it has been shown that the spin-flip probability S_{nn} is, at intermediate energies, a good signature for spin excited states since $S_{nn} \simeq 0$ for ΔS=0 transitions and can reach 0.6 for a ΔS=1 state such as the J^π=1$^+$ 15.1 MeV state in ^{12}C. A signature similar to S_{nn} for deuteron scattering has been reported in Ref. [13]. It should, however, be noted that the spin-transfer probability for a proton projectile is equal to the same observable for the target nucleons, due to the symmetry of the interacting system. This relationship is not so direct for a deuteron projectile; it will be discussed

*Present Address: Los Alamos National Laboratory, Los Alamos, NM 87545.

in a forthcoming paper.

Following the Madison convention [17] and the formalism of Ohlsen [18], we recall the definition of the observables for a vector- and tensor-polarized deuteron beam along the y axis normal to the scattering plane: A_y and A_{yy} are the vector and tensor analyzing powers of the reaction, $P^{y'}$ and $P^{y'y'}$ are the vector and tensor polarizing powers of the reaction, and $K_y^{y'}$ and $K_{yy}^{y'y'}$ the vector and tensor spin-transfer coefficients (the lower indices refer to the incident-beam frame; the upper to that of the scattered beam).

For a deuteron beam, three spin-flip probabilities S_0, S_1, and S_2 may be defined; they are the probabilities for a change of 0, 1, or 2 units of the spin projection along the y axis. The S_1 probability is similar to S_{nn} in $(\vec{p},\vec{p}')$ scattering.

$$S_0 = \frac{1}{6}(2 + 3K_y^{y'} + K_{yy}^{y'y'}), \tag{2.1}$$

$$S_1 = \frac{1}{9}(4 - A_{yy} - P^{y'y'} - 2K_{yy}^{y'y'}), \tag{2.2}$$

$$S_2 = \frac{1}{18}(4 + 2A_{yy} - 9K_y^{y'} + 2P^{y'y'} + K_{yy}^{y'y'}). \tag{2.3}$$

It has been shown [18] that in the plane wave approximation, S_1=0 for ΔS=0 transitions. As for S_{nn} in $(\vec{p},\vec{p}')$, it is expected that S_1 remains small for ΔS=0 transitions, even in the presence of distortion. For ΔS=1 transitions S_1 is expected to be positive. For pure ΔS=0 states we necessarily have $S_2 = 0$ and $A_{yy} = P^{y'y'}$. For other transitions, in a one-step process, S_2=0 if only the S state of the deuteron is considered and if the effective interaction is obtained from the N-N interaction by a folding procedure. By assuming that $A_{yy} = P^{y'y'}$ is still valid, and that $S_2 = 0$, we can derive the following expression for S_1, called from now on S_d^y :

$$S_d^y = \frac{4}{3} + \frac{2}{3}A_{yy} - 2K_y^{y'}. \tag{2.4}$$

The only polarization measurement in the focal plane of the spectrometer required to determine S_d^y is the vector-depolarization coefficient $K_y^{y'}$. Tensor polarization transfer measurements are much more time consuming. The only tensor quantity required for S_d^y is A_{yy}, an analyzing power which can be measured easily.

A. Microscopic description of deuteron-nucleus scattering

It has been shown in a previous $(\vec{d},d')$ experiment at 400 MeV [19] that the angular distribution of the vector analyzing power A_y for different transitions in different nuclei, when plotted as a function of q, is very similar to that measured in 200 MeV $(\vec{p},p')$ scattering. This is one indication that it is reasonable to assume that $(\vec{d},d')$ scattering at 400 MeV is dominated by one-step N-N interactions and can be described in first order by the impulse approximation like 200 MeV protons.

The free nucleon-nucleon (N-N) scattering amplitude, $M(E,q)$, at an incident energy E and for a momentum transfer q, is usually written in the coordinate system of Wolfenstein as

$$M(E,q) = \mathcal{A} + \mathcal{B}\,\sigma_{i\hat{n}}\,\sigma'_{j\hat{n}} + \mathcal{C}(\sigma_{i\hat{n}} + \sigma'_{j\hat{n}}) + \mathcal{E}\sigma_{i\hat{q}}\sigma'_{j\hat{q}} + \mathcal{F}\sigma_{i\hat{p}}\sigma'_{j\hat{p}}, \tag{2.5}$$

where $\mathcal{A}$, $\mathcal{B}$, $\mathcal{C}$, $\mathcal{E}$, and $\mathcal{F}$, which are functions of q and of the isospin transfer τ, are deduced from the Arndt phase shifts [20]. The indices i and j stand for the incident nucleon and the target nucleon, respectively. Here it is convenient to express $M(E,q)$ in a standard basis [21] as

$$M_0(E,q) = \sum_{\lambda\lambda'\nu\nu'} d_{\nu\nu'}^{\lambda\lambda'}(\tau = 0)\sigma^{\lambda}\sigma^{\lambda'} \tag{2.6}$$

for the isoscalar part and

$$M_1(E,q) = \sum_{\lambda\lambda'\nu\nu'} d_{\nu\nu'}^{\lambda\lambda'}(\tau = 1)\sigma^{\lambda}\sigma^{\lambda'}\boldsymbol{\tau}_i \cdot \boldsymbol{\tau}_j \tag{2.7}$$

for the isovector part. The $d_{\nu\nu'}^{\lambda\lambda'}(\tau)$ are linear combinations of the $\mathcal{A}$, $\mathcal{B}$, $\mathcal{C}$, $\mathcal{E}$, and $\mathcal{F}$ terms; σ^{λ} and $\sigma^{\lambda'}$ are spin operators for a spin transfer $\Delta S = \lambda$ in the projectile and $\Delta S = \lambda'$ in the target, respectively.

If we assume that, for the reaction $A(a,b)B$, the deuteron-nucleus interaction is the sum of the interactions of each nucleon of the deuteron with each nucleon of the nucleus, then the deuteron-nucleus amplitude is proportional to

$$2\sum_{m_b' m_a'} \int \chi^{(-)*}_{m_b m_b'}(\mathbf{r},\mathbf{k}_b)\ \mathcal{Z}\ \chi^{(+)}_{m_a m_a'}(\mathbf{r},\mathbf{k}_a)d\mathbf{r}\,d\mathbf{q} \tag{2.8}$$

with

$$\mathcal{Z} = \langle \Phi^{m_b'}_{s_b}(\xi_1,\xi_2,\mathbf{r}_{12})\Psi^{M_B}_{J_B} | \sum_j M_0(E,q) e^{i\mathbf{q}(\mathbf{r}-\boldsymbol{\rho}_j - \mathbf{r}_{12}/2)} | \Psi^{M_A}_{J_A}\Phi^{m_a'}_{s_a}(\xi_1,\xi_2,\mathbf{r}_{12})\rangle. \tag{2.9}$$

Here the sum runs over all the nucleons in the nucleus. The isoscalar part $M_0(E,q)$ of the free N-N scattering amplitudes is taken at an energy $E = E_{\text{deuteron}}/2$.

$\Phi^{m_a'}_{s_a}(\xi_1,\xi_2,\mathbf{r}_{12})$ and $\Phi^{m_b'}_{s_b}(\xi_1,\xi_2,\mathbf{r}_{12})$ are the deuteron wave functions in the incoming and outgoing channels, respectively, as a function of the internal coordinates ξ_1 and ξ_2 of the nucleons in the deuteron and their separation $\mathbf{r}_{12}$; the deuteron wave function calculated from the Paris potential [22] (94.3% S state and 5.7% D state) is used. $\Psi^{M_A}_{J_A}$ and $\Psi^{M_B}_{J_B}$ are the nuclear wave functions for the target and residual nucleus; $\mathbf{r}$ is the distance between the center of mass of the deuteron and the center of mass of the nucleus; $\boldsymbol{\rho}_j$ is the distance of the struck nucleon in the nucleus to the center of mass of the nucleus. All the

calculations in the present paper were performed in plane waves, so the momentum transfer $\mathbf{q} = \mathbf{k}_b - \mathbf{k}_a$, the χ wave functions are simple plane waves, and the summation on m'_a and m'_b disappears.

The spin J_d transferred to the deuteron can be 0, 1, or 2 as $|s_a - s_b| \leq J_d \leq s_a + s_b$. Then three cross sections σ_0, σ_1, and σ_2 can be associated with these transfers, and three ratios Π_0, Π_1, and Π_2 can be defined as

$$\Pi_{J_d} = \frac{\sigma_{J_d}}{\sum_{J_d} \sigma_{J_d}}. \tag{2.10}$$

For the target nucleon there are only two possible values for the spin transfer: 0 or 1. Thus we can similarly define two cross sections and two ratios, Π'_0 and Π'_1. It should be noted that the signatures S_0, S_1, and S_2 defined above give the probability that the projection of the deuteron spin changes by 0, 1, or 2 units, while the ratios Π_{J_d} give the probability that J_d units of spin itself are transferred.

It can be shown that $S_d^y = S_1 + 4S_2$ if $A_{yy} = P^{y'y'}$ (which is true for the scattering from a free nucleon). If the D state is omitted in the deuteron wave function, $S_2 = 0$ and S_d^y is equal to S_1. For a 400 MeV deuteron scattering on a free nucleon, the signatures S_1 and S_d^y, plotted in Fig. 1, are very close in the range of the present experiment ($q < 1$ fm^{-1}). In this range of momentum transfer the non-spin-flip part of the interaction dominates (see Fig. 2), giving values for S_d^y smaller than 0.1.

Let σ_{00}^A and σ_{10}^A be the isoscalar cross sections for a spin transfer of 0 and 1 to the nucleus. Following the method given in Ref. [14] for $(\vec{p}, \vec{p}')$ scattering, we can define an α^A coefficient by

$$S_d^y = (\sigma_{10}^A \, \alpha^A)/(\sigma_{00}^A + \sigma_{10}^A). \tag{2.11}$$

For a pure ΔS=1 transition ($\sigma_{00}^A = 0$), $\alpha^A = S_d^y$.

By making the same approximations as in $(\vec{p}, \vec{p}')$ [14] and assuming that these approximations are valid in the same range of momentum transfer in the present experiment, we can replace α^A by α^{free} calculated in the free

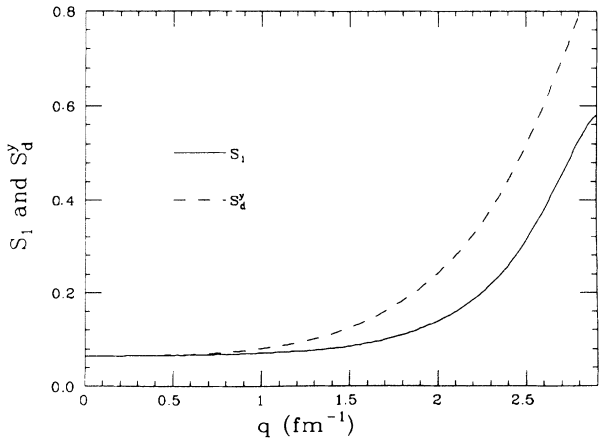

FIG. 1. S_1 and S_d^y calculated with the free deuteron-nucleon interaction as a function of q (fm^{-1}).

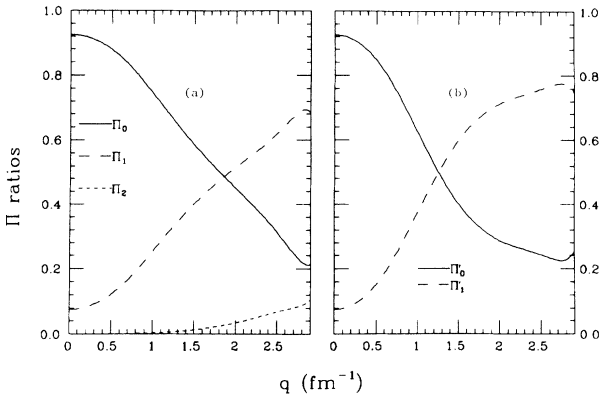

FIG. 2. Π ratios. (a) For the deuteron projectile; (b) for the target nucleon as a function of q (fm^{-1}).

deuteron-nucleon (d-N) scattering and factorize the cross sections as

$$\sigma_{i0}^A = N_{\text{eff}} \; f_{i0} \; \sigma_{i0}^{\text{free}}. \tag{2.12}$$

Here N_{eff} is the effective number of participating nucleons (supposed to be the same in both channels), f_{i0} the isoscalar nuclear response in the spin channel i, and $\sigma_{i0}^{\text{free}}$ the d-N scattering cross section calculated for the q value of the deuteron nucleus inelastic scattering. Then

$$S_d^y = (f_{10} \; \sigma_{10}^{\text{free}} \; \alpha^{\text{free}})/(f_{10} \; \sigma_{10}^{\text{free}} + f_{00} \; \sigma_{00}^{\text{free}}) \tag{2.13}$$

with $\alpha^{\text{free}} = S_d^y(\text{free})/\Pi'_1(\text{free})$.

This factorization method is a rough approximation expected to be valid at high energy loss and for q less than 1 fm^{-1}. For a state whose structure is known, the calculation can be performed without this approximation.

The relative isoscalar spin response is defined as

$$R_S^0 = \frac{f_{10}}{f_{10} + f_{00}} \tag{2.14}$$

in analogy with the corresponding isospin-averaged quantity R_S measured in proton scattering. With the above factorization approximation, and with the assumption that distortion corrections are the same in both spin channels,

$$R_S^0 = \frac{S_d^y(\text{measured}) \; \Pi'_0(\text{free})}{S_d^y(\text{measured})\left[\Pi'_0(\text{free}) - \Pi'_1(\text{free})\right] + S_d^y(\text{free})} \tag{2.15}$$

where $\Pi'_0(\text{free})$ and $\Pi'_1(\text{free})$ are calculated for deuteron scattering on a free nucleon. In Fig. 3 R_S^0 is plotted as a function of S_d^y for q =0.5 fm^{-1}. For small S_d^y values, the slope of the curve is large, leading to a large uncertainty on R_S^0.

From the above relations

$$\sigma_{10}^A = \frac{1}{\alpha^{\text{free}}} \frac{d\sigma}{d\Omega} S_d^y(\text{measured}), \tag{2.16}$$

where $\frac{d\sigma}{d\Omega} = \sigma_{00}^A + \sigma_{10}^A$ is the experimental cross section.

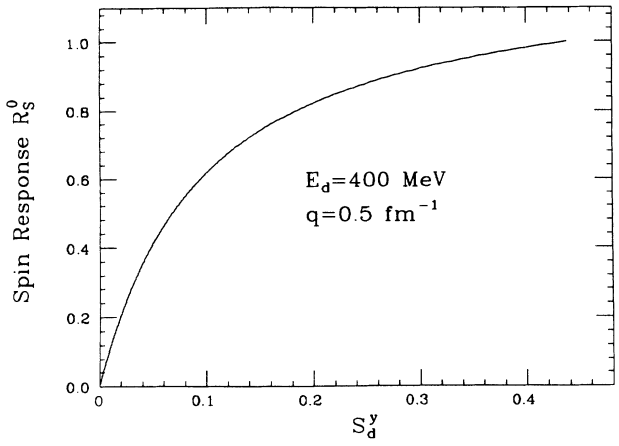

FIG. 3. Spin response R_S^0.

III. EXPERIMENTAL SET-UP AND PROCEDURE

The measurements were performed with the 400 MeV polarized deuteron beam at the Laboratoire National Saturne (LNS). The data were taken at the high-resolution energy-loss spectrometer SPES1 [23] using the vector polarimeter POMME [24,25] and the acquisition system described in Ref. [26]. The thicknesses of the carbon scatterer and of the iron absorber that gave the best figure of merit [25] for 400 MeV deuterons were respectively 7.2 and 4.1 cm. A schematic view of the experimental setup is given in Fig. 4. Using a 44 mg/cm^2 ^{12}C or a 46.5 mg/cm^2 ^{40}Ca target the energy resolution was 200 keV (FWHM). Good background rejection was obtained by setting horizontal and vertical windows on target and focal-plane variables of the scattered deuterons.

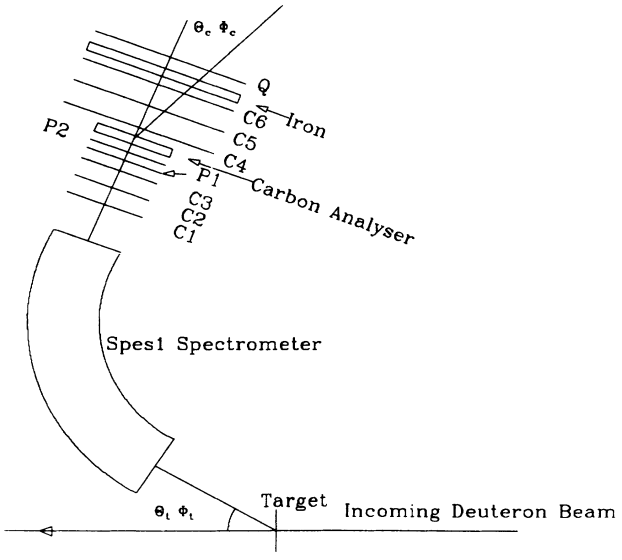

FIG. 4. Experimental setup.

A. The deuteron polarized beam

Two different types of polarized deuteron beam were used. In the first mode, the beam is vector and tensor polarized, in four different states labeled 5, 6, 7, and 8 in the notation of [27]. The polarization state changed with each beam pulse. The vector and tensor polarizations p_z and p_{zz} in this reference become p_y and p_{yy} in the Madison convention used for our experiment. The p_y and p_{yy} values were measured regularly with the low-energy polarimeter [27]. They were found to be stable within a statistical uncertainty of 3% and equal to $p_y = 0.312 \pm 0.010$ (giving a polarization efficiency of 93.6%) and $p_{yy} = 0.830 \pm 0.020$ (83% efficiency), the errors being only statistical. An absolute uncertainty of 2.5% comes from the calibration of the low-energy polarimeter; furthermore, a correction for the dead time of its electronics must be added [28].

This polarized beam has been used to measure

$$A_y = (2/3p_y)(N_5 - N_6 + N_7 - N_8)/(N_5 + N_6 + N_7 + N_8), \tag{3.1}$$

$$A_{yy} = (2/p_{yy})(N_5 + N_6 - N_7 - N_8)/(N_5 + N_6 + N_7 + N_8), \tag{3.2}$$

and

$$A_0 = (N_5 - N_6 - N_7 + N_8)/(N_5 + N_6 + N_7 + N_8), \tag{3.3}$$

where N_5, N_6, N_7, and N_8 are the counts for each of the four states of polarization of the deuteron beam. Due to the polarization of the beam in each state [27], A_0 must be zero.

In the second mode, the beam is only vector polarized, with states 2 and 3 of Ref. [27]. The p_y value was regularly measured and found equal to 0.598 ± 0.008, thus giving a polarization efficiency of 89.7%. With this beam

$$A_y = (2/3p_y)\frac{N_3 - N_2}{N_3 + N_2}. \tag{3.4}$$

B. Tests of the beam polarization and of the polarimeter POMME

As a test of the accuracy of the beam polarization measurement and of the POMME calibration, time-reversal invariance properties in elastic scattering $A_y = P^{y'}$ and $S_d^y = S_1 = 0$ were checked in ^{40}Ca at 6°. In order to satisfy these equations, the beam polarization had to be renormalized by 1.040 ± 0.005 and the analyzing power of POMME divided by 1.045 ± 0.005. These corrections were traced to dead-time corrections in the electronics of the low-energy polarimeter which were not included during the POMME calibration [28]. These new values are used for the analysis of the present data. We also checked that A_y as measured with the 2-state beam was the same as A_y measured with the 4-state beam, and that it was

independent of whether or not the focal-plane polarimeter was included in the trigger.

The spatial extension of the focal plane of the spectrometer which can be used with the polarimeter POMME was determined by setting the elastic peak at different positions in the focal plane. For each position it was verified that A_y remained constant (A_y=0.603 ± 0.006) and equal to $P^{y'}$ (0.593 ± 0.008) measured at the same time and that S_d^y is consistent with 0 (0.017 ± 0.020). It is then deduced that, for a deuteron energy of 400 MeV, POMME may be used for an excitation energy range of 19 MeV, the systematic error on S_d^y being less than 0.02.

C. Experimental method

The measurements were performed in two steps. First the four-state vector- and tensor-polarized beam was used to measure the cross sections and the vector and tensor analyzing powers A_y and A_{yy}, using only the first three proportional wire chambers C1, C2, and C3 of POMME triggered by the P1 and P2 plastic scintillators (see Fig. 4). The intensity of the beam was measured with two monitors M1 (located at an angle of 60° in the vertical plane) and M2 (located in the scattering plane at an angle of 45°). It was verified that the ratio of the counting rates of the monitors remained constant to ±6% during the whole experiment. The absolute calibration of these monitors was performed with the carbon activation method [29].

Accounting for the uncertainties in the activation analysis and the efficiency of the wire chambers, the absolute error on the cross sections is estimated to be ± 15%. As a test of the corrections on the electronic dead time, it has been verified that A_0=0 within the statistical uncertainty of ± 0.004.

In the second step, the vector-polarized deuteron beam was used, essentially because the value of p_y is twice as large as the value that could have been obtained with the four-state polarized beam. Moreover, the $p_{y'}$ values are measured with a statistical error half of that which would have been obtained in a four-state measurement in a comparable time. To reject the Coulomb multiple scattering in the carbon block, only particles scattered at an angle larger than 4.5° were accepted. Accounting for the angular acceptance of POMME, the efficiencies of the rear wire chambers, and the different tests on the events, the total efficiency of the polarimeter is about 2.5%. This efficiency is shown in Fig. 5 as a function of the difference between the energy of the scattered particles and the central rays. The shape of the curve is essentially due to geometrical effects of the "cone test" rejection [30].

Measurements of $K_y^{y'}$ and of the signature S_d^y were also performed with a four-state vector- and tensor-polarized deuteron beam; the results were consistent with those obtained with the two-state polarized beam. As all the relations between $p_{y'}$ and the observables $P^{y'}$ and $K_y^{y'}$ are different in the two cases, we are made confident about the method.

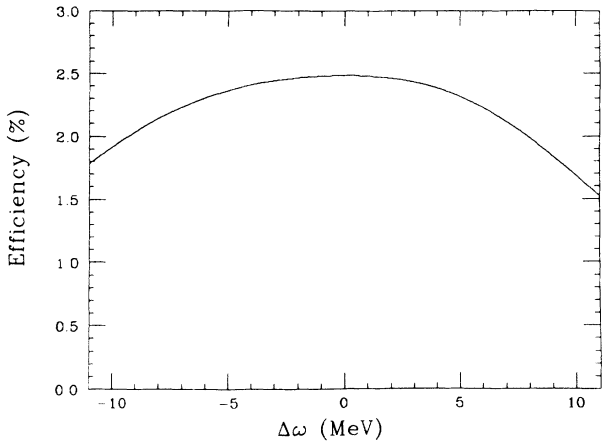

FIG. 5. Detection efficiency of the polarimeter POMME along the focal plane of the spectrometer (see text).

D. Extraction of the $P^{y'}$ and $K_y^{y'}$ values

The $K_y^{y'}$ and $P^{y'}$ values are related to A_y and to the polarization of the scattered beam $p_{y'}^{\uparrow}$ and $p_{y'}^{\downarrow}$ for the two states of polarization 3(↑) or 2(↓) of the incident beam as follows:

$$K_y^{y'} = \frac{1}{3p_y}[p_{y'}^{\uparrow} - p_{y'}^{\downarrow} + \tfrac{3}{2}p_y A_y(p_{y'}^{\uparrow} + p_{y'}^{\downarrow})], \tag{3.5}$$

$$P^{y'} = \frac{1}{2}[p_{y'}^{\uparrow} + p_{y'}^{\downarrow} + \tfrac{3}{2}p_y A_y(p_{y'}^{\uparrow} - p_{y'}^{\downarrow})]. \tag{3.6}$$

The analysis of the data to extract the values of $p_{y'}^{\uparrow}$ and $p_{y'}^{\downarrow}$ was done in the following way. Each event was stored in a multiparameter spectrum as a function of the beam polarization state, of the excitation energy ω in the target (in 0.1 MeV bins), of the target scattering angle Θ_t (in 0.1° bins), and of the polar and azimuthal scattering angles Θ_c and Φ_c in the carbon analyzer (in 1° and 10° bins, respectively) for Θ_c between 4.5° and 19.5°. For each value of ω, Θ_t, and polarization state, a two-dimensional spectrum $N(\Theta_c,\Phi_c)$ was plotted. The origin of Φ_c is taken in the scattering plane of the first reaction. For each value of Θ_c, $N(\Theta_c, \Phi_c)$ is expanded as a function of Φ_c:

$$N(\Theta_c, \Phi_c) = N_0(\Theta_c)[1 + a\cos(\Phi_c) + b\cos(2\Phi_c) + c\sin(\Phi_c) + d\sin(2\Phi_c)]. \tag{3.7}$$

Due to the symmetry of the incident beam, the coefficients c and d should be zero; they were evaluated by a Fourier analysis of the $N(\Theta_c, \Phi_c)$ distribution and were generally found to be compatible with zero. In the cases where those values were not zero, the measure was rejected. The coefficients $N_0(\Theta_c)$, a and b, were extracted by a χ^2 minimization method with $c = d = 0$ for each polarization state of the beam and each Θ_c bin.

The parameter a is directly related to the vector polarization of the scattered deuterons:

$$p_{y'} = -\frac{1}{\sqrt{3}}\frac{a}{iT_{11}}, \tag{3.8}$$

where iT_{11} is the vector analyzing power of the polarimeter [25] at the energy $E_{\rm inc}-\omega$ for the scattering angle Θ_c. The weighted average of the results so obtained gives the final polarization $p_{y'}$ inserted in the above formulas.

When the cross sections were extracted from the measurements performed with the whole POMME setup, they were corrected by the efficiency of the polarimeter as given in Fig. 5.

IV. EXPERIMENTAL RESULTS AND DISCUSSION

A. Test of the signature in $(\vec{d},\vec{d}')$ scattering on ^{12}C

The first results on ^{12}C reported in Ref. [13] have to be slightly modified due to the reanalysis of the data with the corrected values for the incident beam polarization and for the POMME analyzing power. For the ΔS=0 states we get A_y=$P^{y'}$ (to an accuracy of ± 0.023 for the 2^+ state) as predicted by plane wave calculations using the Cohen-Kurath wave functions [31]. In these calculations for ΔS=1 states we obtained A_{yy}=$P^{y'y'}$, supporting our approximation $S_1 = S_d^y$.

The results on ^{12}C obtained at 4° are plotted in Fig. 6 as a function of the excitation energy. The signatures for the ΔS=0 states at 4.44, 7.65, and 9.64 MeV are compatible with zero, while the ΔS=1, 1^+ state at 12.71 MeV and the 2^- state at 18.3 MeV have strong signatures. In Table I the experimental values of S_d^y at 4° and 6° for four states are given, and the values are evaluated in the impulse approximation as described in Sec. II A. The ^{12}C wave functions for the different excited states were taken from Ref. [31]. The values of the spin response R_S^0 are also given for the 12.71 MeV state.

Equation (2.13) can be used to predict the value of S_d^y in the plane wave limit for a pure spin-flip transition ($f_{00}=0, f_{10}=1$): S_d^y=$\alpha^{\rm free}$. The excitation of the 12.7 MeV state at 4° corresponds to a momentum transfer q = 0.465 fm^{-1} and leads to S_d^y=0.48. This value is in very good agreement with S_d^y=0.47 calculated using the Cohen-Kurath wave function. These nearly identical values confirm the validity of the approximation $\alpha^A = \alpha^{\rm free}$.

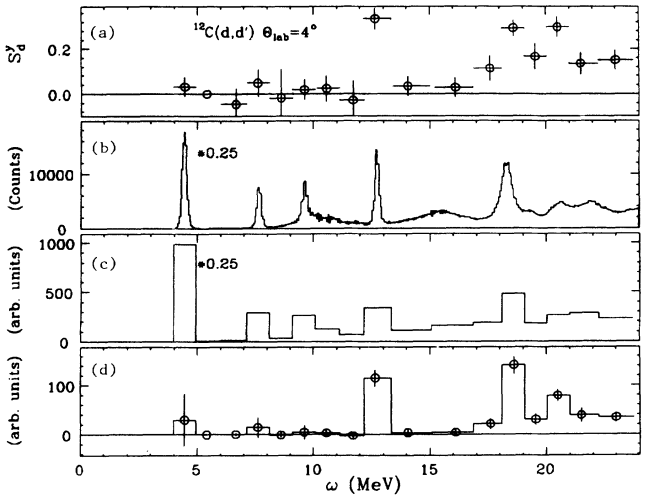

FIG. 6. Results on ^{12}C at 4° lab as a function of the excitation energy. (a) The S_d^y signature; (b) spectrum in 100 keV bins; (c) same spectrum summed over 500 keV bins; and (d) product $(d\sigma/d\Omega\, dE)S_d^y$ (in arbitrary units).

From Eq. (2.15) R_S^0=0.94±0.03 for the 4° experimental value S_d^y=0.33±0.05. This can be explained by a small non-spin-flip continuum underlying the 12.71 MeV peak.

B. The ^{40}Ca nucleus

The spin signature S_d^y was measured at the laboratory scattering angles of 4° and 6° (from q = 0.28 to q = 0.8 fm^{-1}), each measurement covering an angular range of ±1°. Use of two different magnetic field settings permitted the study of excitation energies from 6.25 to 42 MeV. There is no background at the low-energy setting and less than 7% in the 24 to 42 MeV range. At 6° and 8° the signature cancellation was checked on the 3.74 MeV 3^- level to an accuracy of ±0.04; this shows that distortion effects on ΔS=0 transitions may still be neglected for ^{40}Ca at q = 0.9 fm^{-1}.

The results were extracted at 4° and 6° in 1 MeV bins between 6.25 and 10.5 MeV, in 1.5 MeV bins up to 12 MeV and in 2 MeV bins between 12 and 42 MeV. The signatures S_d^y are shown in Fig. 7 for 4° and 6°. The errors include the statistical uncertainty which comes es-

TABLE I. Signature for the three ΔS=0 states 2^+, 0^+, 3^- and for the spin-flip state at 12.71 MeV in ^{12}C measured at Θ = 4° and 6°. The theoretical values for S_d^y are calculated using the model of Ref. [31].

	Experimental		Theoretical		R_S^0 Response	
ω (MeV)	4°	6°	4°	6°	4°	6°
4.44	0.03±0.04	-0.01±0.04	0.002	0.004		
7.65	0.05±0.06	-0.06±0.05				
9.64	0.02±0.04	0.03±0.03	0.001	0.002		
12.71	0.33±0.05	0.30±0.05	0.472	0.299	0.94±0.03	0.99±0.03

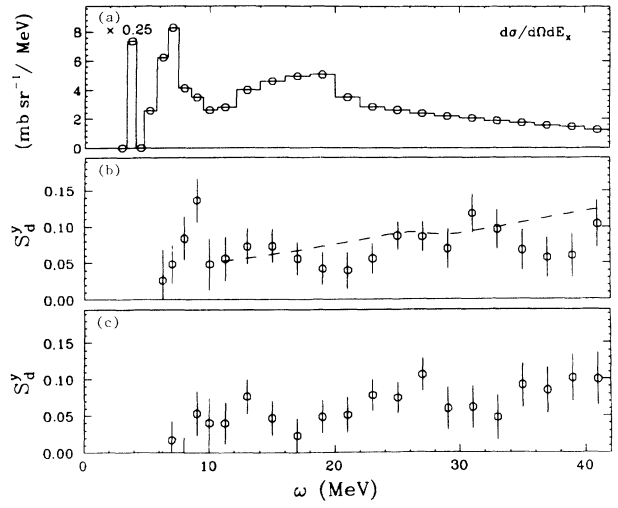

FIG. 7. Experimental data on ^{40}Ca. (a) Spectrum at 6°. (b) Signature S_d^y at 4°. The curve (dashed line) is the isoscalar spin signature as calculated in Ref. [33] for 319 MeV protons. (c) Signature S_d^y at 6°.

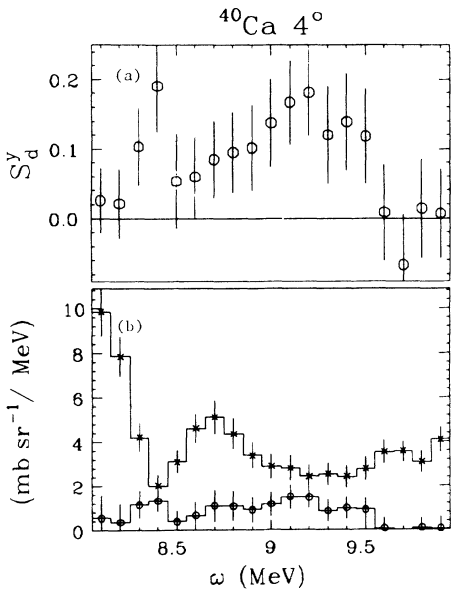

FIG. 8. Excitation energy region from 8 to 10 MeV studied in 100 keV energy bins for $3° < \Theta_t < 5°$. (a) Signature. (b) Spin cross sections (open circles) and non-spin cross sections (crosses).

sentially from the uncertainty on $K_y^{y'}$. The absolute uncertainties on the vector and tensor polarization of the beam are also included in the error bars. The strongest signature is seen in the 9 MeV region at 4° where it reaches about 0.13. Values elsewhere range between about 0.05 and 0.10 at both angles. Except at the lowest energies, these values are much lower than the values of S_{nn} measured in $(\vec{p},\vec{p}')$ at 319 MeV, where the values reached about 0.40 at 40 MeV. But they are comparable with the free values of S_d^y shown in Fig. 1, and they suggest the presence of a broad distribution of ΔS=1, ΔT=0 strength over this region.

Because of the statistical errors on S_d^y, smaller energy and angular bins cannot be studied simultaneously. The excitation energy region from 8 to 10 MeV has been studied in 100 keV bins for $3° < \Theta_t < 5°$. The results are plotted in Fig. 8; two maxima of S_d^y appear at 8.4 and 9.2 MeV with R_S^0 values of 0.8. The spin-flip cross section for a 2 MeV bin centered at 9 MeV, given in Fig. 9, is compatible with the angular distribution of a 2^- state; the calculations were performed in plane wave impulse approximation with the wave functions of the two main 2^- states predicted by Brown [32] which give the same shape. Nevertheless, in this case, the shape of the angular distribution is not enough to unambiguously determine the J^π nature of this structure. However, the large values of R_S^0 in this energy region strongly suggest the presence of significant isoscalar spin-flip strength which was unknown until now.

Brown [32] predicted strong 2^-, $T = 0$ states at 6.77 and 11.606 MeV and several others around 15 MeV. The computed values for S_d^y are about 0.5, close to the expected value for a pure spin-flip transition obtained using Eq. (2.13). Unkelbach and Wambach [33] have calculated the cross sections and S_{nn} values for the scattering of 319 MeV protons at 7° (q=0.53 fm^{-1}) on ^{40}Ca. They also found a strong isoscalar 2^- state at 7 MeV and two other weak states near 8 MeV. Although the present measurements cover the excitation energy region between 6 and 8 MeV, the small values of S_d^y due to the large excitation of known ΔS=0 states do not allow us to draw any conclusions regarding the presence of narrow

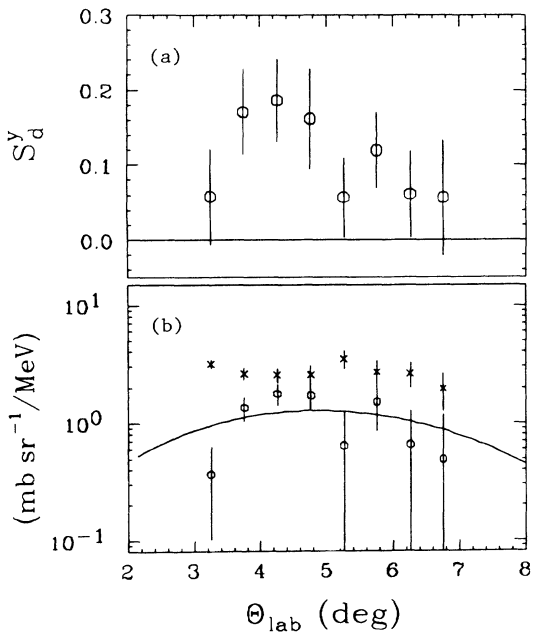

FIG. 9. Angular distribution for ω between 8 and 10 MeV. (a) For S_d^y; (b) for the spin cross sections (open circles) and nonspin cross sections (crosses). The angular distribution plotted (solid line) is for the 2^- state at 6.77 MeV [32] normalized to the experimental data.

spin-flip states in this region.

For the region of the continuum, the R_S^0 values and the σ_{00}^A and σ_{10}^A cross sections are given as functions of ω at 4° and 6° in Figs. 10 and 11, respectively. The difference in the spin-flip strength distribution shown in these figures is due to a faster decrease of the measured spin-flip cross section in the lower excitation energy region and the large binning in angle (±1°) used to produce these figures. The analysis of the data was done with smaller angular bins (±0.25°) and showed a smooth angular dependence for the spin-flip strength distribution. As expected the giant quadrupole resonance appears near 18 MeV in the σ_{00}^A cross section. At 4°, there is a concentration of spin strength with a maximum near 15 MeV and then the strength is spread between 20 and 42 MeV. These results are in qualitative agreement with the predictions of Ref. [33]: 2^- states are predicted between 13 and 20 MeV and 3^+ states are essentially localized between 20 and 33 MeV. In Fig. 7(b) our experimental S_d^y values at 4° are compared with the isoscalar spin-flip probabilities calculated in Ref. [33] simply by switching off the ΔT=1 strength in the theoretical calculation of S_{nn}. This comparison is not unreasonable because the α^{free} obtained in d-N at 400 MeV is close to α^{free}= 0.49 obtained in p-N at 319 MeV. The isoscalar spin-strength distribution is well predicted. The attenuation due to the giant quadrupole resonance around 20 MeV seems to be underestimated, and, in contrast to the proton results, the experimental spin strength is weaker than the one predicted between 35 and 40 MeV. This comparison, which neglects the difference between distortions in the two channels, is another indication of the apparent simplicity in the interpretation of these spin-transfer experiments.

The angular distribution of σ_{10}^A for 2 MeV bins centered at 15, 27, and 35 MeV is given in Fig. 12; there is a slight shift of the maximum to larger scattering angles

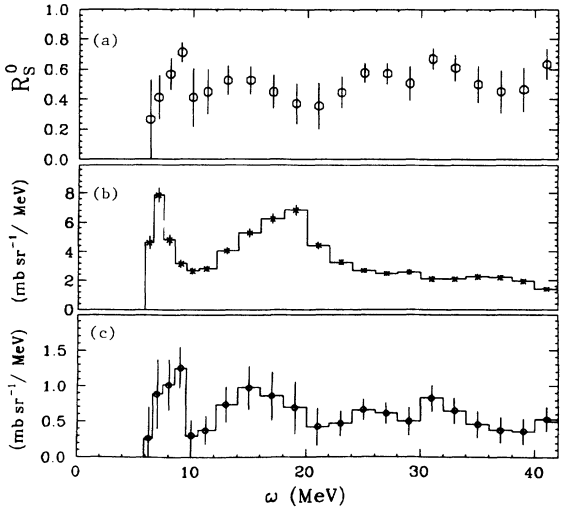

FIG. 10. Results extracted on ^{40}Ca at 4°. (a) Spin response R_S^0. (b) Nonspin cross section. (c) Spin cross section.

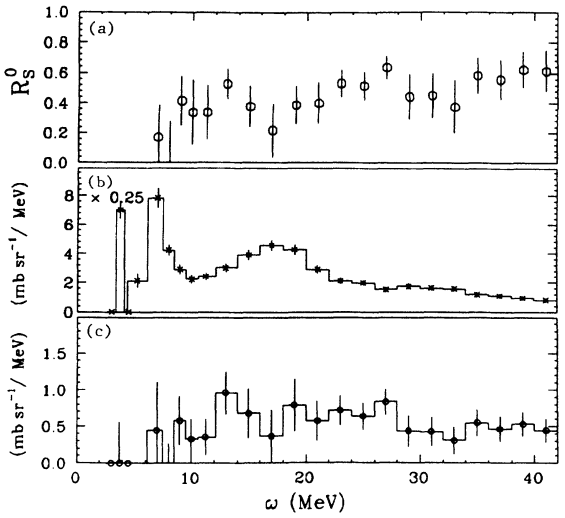

FIG. 11. Results extracted on ^{40}Ca at 6°. (a) Spin response R_S^0. (b) Nonspin cross section. (c) Spin cross section.

when ω increases, suggestive of the presence of higher multipolarities at higher ω.

The $(\vec{p},\vec{p}')$ experiments performed at 319 MeV on ^{40}Ca [14] at $q \simeq 0.5\,\text{fm}^{-1}$ give the total spin response denoted R_S. The spin responses f_0 and f_1 defined in Ref. [14] are averages over isospin:

$$f_i = \frac{f_{i1}\sigma_{i1}^{\text{free}} + f_{i0}\sigma_{i0}^{\text{free}}}{\sigma_{i1}^{\text{free}} + \sigma_{i0}^{\text{free}}}, \tag{4.1}$$

where the first index indicates the spin channel and the second index the isospin channel, the $\sigma_{ij}^{\text{free}}$ being proton-nucleon cross sections,

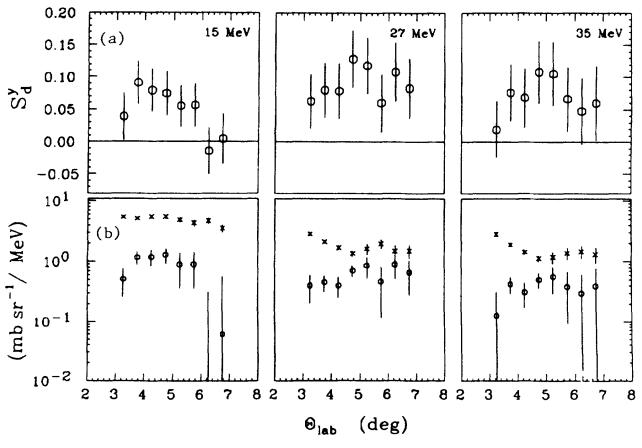

FIG. 12. Angular distribution. (a) For S_d^y; (b) for the spin (circles) and nonspin (crosses) cross sections for 2 MeV energy bins centered at 15, 27, and 35 MeV.

$$R_S = \frac{\frac{\sigma_{11}^{\text{free}}}{\sigma_1^{T\ \text{free}}}\left(1+\frac{\sigma_{10}^{\text{free}}}{\sigma_{11}^{\text{free}}}\frac{f_{10}}{f_{00}}\frac{f_{00}}{f_{11}}\right)}{\frac{\sigma_{11}^{\text{free}}}{\sigma_1^{T\ \text{free}}}\left(1+\frac{\sigma_{10}^{\text{free}}}{\sigma_{11}^{\text{free}}}\frac{f_{10}}{f_{00}}\frac{f_{00}}{f_{11}}\right)+\frac{\sigma_{00}^{\text{free}}}{\sigma_0^{T\ \text{free}}}\left(\frac{f_{00}}{f_{11}}+\frac{\sigma_{01}^{\text{free}}}{\sigma_{00}^{\text{free}}}\frac{f_{01}}{f_{11}}\right)} \tag{4.2}$$

with $\sigma_i^{T\ \text{free}} = \sigma_{i0}^{\text{free}} + \sigma_{i1}^{\text{free}}$.

Each σ_{ij} can be calculated exactly; $\sigma_{01}^{\text{free}}/\sigma_{00}^{\text{free}}$ is small and nearly constant between 319 and 800 MeV (0.039 and 0.032, respectively, at $q = 0.5\,\text{fm}^{-1}$). It may be shown that $(\sigma_{01}^{\text{free}}/\sigma_{00}^{\text{free}})(f_{01}/f_{11})$ can be neglected if f_{01} is smaller than half the total strength. With this condition the second term in the denominator is $(f_{10}/f_{11})(f_{00}/f_{10})$.

For given values of the f_{ij} and for different momentum transfers, the energy dependence of R_S on the $\sigma_{ij}^{\text{free}}$ cross sections is predicted to be very weak as found experimentally [34]: R_S(800 MeV)/R_S(319 MeV) is 0.98 for q=0.5 fm^{-1} and 0.94 for $q = 0.9\ \text{fm}^{-1}$.

The ratio f_{10}/f_{00} obtained from the R_S^0 values measured in the present experiment is shown in Fig. 13(a); the values f_{11}/f_{00} and f_{10}/f_{11} deduced from R_S and R_S^0 are shown in Figs. 13(b) and 13(c), respectively. The ratio f_{11}/f_{00} increases with ω showing a very important contribution of the isovector spin strength at high excitation energies. The ratio f_{10}/f_{00} is essentially equal to one at all excitations energies as expected for a noninteracting isoscalar Fermi gas. The small decrease in the value of this ratio around 20 MeV is due to the excitation of the giant quadrupole resonance in the f_{00} channel. This shows that the collective effects in the continuum are much weaker in the isoscalar channel than in the isovector one. Up to 18 MeV the ratio f_{10}/f_{11} is compatible with one and decreases beyond this energy. For ω greater than 30 MeV, where R_S was found to be larger than 80%, the isoscalar spin strength is less than 25% of the total spin strength.

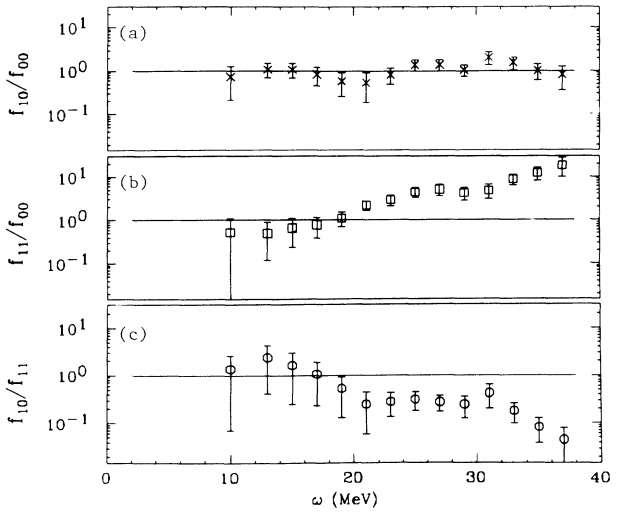

FIG. 13. Relative spin strengths. (a) f_{10}/f_{00} extracted from the present $(\vec{d},\vec{d}')$ data. (b) f_{11}/f_{00} obtained using the relative spin responses R_S^0 (present data) and R_S [$(\vec{p},\vec{p}')$ at 319 MeV]. (c) f_{10}/f_{11} ratio of the ΔT=0 to the ΔT=1 strength in the spin channel.

V. CONCLUSIONS

This first exploration of the isoscalar spin response of a nucleus via the measurement of S_d^y in 400 MeV deuteron scattering on ^{40}Ca has yielded many interesting features. As predicted, the measured values of the spin-flip probability are smaller than for proton-induced reactions, and, as a consequence, they may be more affected by experimental systematic errors or theoretical uncertainties. Nevertheless, the results clearly show the presence of the isoscalar spin component of the nuclear force. In particular, localized isoscalar spin strength was observed in the 9 MeV region. A wide bump located around 15 MeV is roughly 60% spin strength; its angular distribution is consistent with preliminary calculations for a spin-dipole excitation. Little significant structure was observed in the spin-flip cross section at higher energies. The signature S_d^y was roughly consistent with its free value in this region. A simple interpretation of the results suggests a lack of collectivity in this channel which is consistent with previous indications of a weak particle-hole (p-h) force in the ΔS=1, ΔT=0 channel [35], such as the position of the "isoscalar" 1^+ state at 5.845 MeV in ^{208}Pb [36]. On the other hand, it is inconsistent with the calculations of Ref. [37], where the distribution of spin strength was roughly independent of isospin.

In analogy with previous work on spin transfer in proton scattering, a relative spin response R_S^0 was defined. Its values were determined from the S_d^y data with simple assumptions like those made to determine R_S for protons. In contrast to the proton results, where a large enhancement in the spin response relative to the total response was observed at high excitation energy, the values of R_S^0 generally fluctuate around the Fermi-gas value of 0.5. Attempts to explain the proton data have focused on the exhaustion of the ΔS=0 sum rule strength at low excitation energy (thus increasing the relative strength of ΔS=1 at high excitations) and on the repulsive nature of the residual interaction in the ΔS=1, ΔT=1 channel (thus increasing the ΔS=1 strength at high excitation) [38]. The argument based on the exhaustion of ΔS=0 strength would apply equally well here for the deuteron data, predicting an enhancement at high excitation which is not observed. Indeed the various f_{ij} ratios in Fig. 13 suggest that the proton data should be better explained by an enhancement in the spin channel at high excitation. Recent DWIA analysis of measure-

ments of the longitudinal and transverse components of the spin response to protons indicate large corrections in the longitudinal response due to distortions, and the effects on S_{nn} itself [39] are not negligible as previously supposed. This would suggest that R_S might be modified. The distortion corrections are due to both absorption and to the effects of the spin-orbit potential. The effects of distortion on S_d^y have not yet been evaluated in $(\vec{d}, \vec{d}')$ scattering, except, as noted in the text, that S_d^y is experimentally found to be zero for a ΔS=0 transition in ^{40}Ca. In addition, the agreement shown in Fig. 7(b) between the calculation made for the $T = 0$ component of proton scattering with the present deuteron data for S_d^y suggests that distortion corrections should not be very large; however, complete DWIA calculations are needed.

ACKNOWLEDGMENTS

We are grateful to B.A. Brown, W. Unkelbach, and J. Wambach for communicating the results of their model calculations before publication. The technical staff of the Laboratoire National Saturne is acknowledged for its efficient assistance during the experiment. Some of the authors (C.G., B.N.J., F.T.B., D.B., C.D., G.W.R.E., and A.G.) were supported by grants from the U.S. Department of Energy and the National Science Foundation.

[1] Electric and magnetic giant resonances in nuclei, edited by J. Speth (World Scientific, Singapore, in press), and references therein.

[2] J. Rapaport, T. Taddeucci, T. P. Welch, C. Gaarde, J. Larsen, D. J. Horen, E. Sugarbaker, P. Koncz, C. C. Foster, C. D. Goodman, C. A. Goulding, and T. Masterson, Nucl. Phys. **A410**, 371 (1983).

[3] J. Rapaport, R. Alarcon, B. A. Brown, C. Gaarde, J. Larsen, C. D. Goodman, C. C. Foster, D. Horen, T. Masterson, E. Sugarbaker, and T. N. Taddeucci, Nucl. Phys. **A427**, 332 (1984).

[4] J. Watson, B. D. Anderson, and R. Madey, Can. J. Phys. **65**, 566 (1987).

[5] A. Brockstedt, L. Berqgvist, L. Carlen, P. Ekström, B. Jakobsson, C. Ellegaard, C. Gaarde, J. S. Larsen, C. D. Goodman, M. Bedjidian, D. Contardo, J. Y. Grossiord, A. Guichard, J. R. Pizzi, D. Bachelier, J. L. Boyard, T. Hennino, J. C. Jourdain, M. Roy-Stéphan, M. Boivin, T. Hasegawa, and P. Radvanyi, Nucl. Phys. **A530**, 571 (1991).

[6] A. Richter, in *Proceedings of the International Conference on Nuclear Physics*, Florence, Italy, 1983, edited by P. Blasi and R. A. Ricci (Tipografia Compositori, Bologna, 1983), p. 189.

[7] C. Djalali, N. Marty, M. Morlet, A. Willis, J. C. Jourdain, A. Anantaraman, G. M. Crawley, and A. Galonsky, Nucl. Phys. **A388**, 1 (1982).

[8] C. Djalali, Ph.D. Université Paris XI, Orsay, 1984.

[9] F. T. Baker, L. Bimbot, R. W. Fergerson, C. Glashausser, K. W. Jones, A. Green, K. Nakayama, and S. Nanda, Phys. Rev. C **37**, 1350 (1988).

[10] F. T. Baker, L. Bimbot, R. W. Fergerson, C. Glashausser, A. Green, K. Jones, W. G. Love, and S. Nanda, Phys. Rev. C **40**, 1877 (1989).

[11] O. Häusser, M. C. Vetterli, R. W. Fergerson, C. Glashausser, R. G. Jeppesen, R. D. Smith, R. Abegg, F. T. Baker, A. Celler, R. L. Helmer, R. Henderson, K. Hicks, M. J. Iqbal, K. P. Jackson, K. W. Jones, J. Lisantti, J. Mildenberger, C. A. Miller, R. S. Sawafta, and S. Yen, Phys. Rev. C **43**, 230 (1991).

[12] F. T. Baker, L. Bimbot, R. W. Fergerson, C. Glashausser, A. Green, O. Häusser, K. Hicks, K. W. Jones, C. A. Miller, M. C. Vetterli, R. Abegg, D. Beatty, B. Bonin, B. Castel, X. Y. Chen, V. Cupps, C. Djalali, R. Henderson, K. P. Jackson, R. G. Jeppesen, K. Nakayama, S. K. Nanda, R. S. Sawafta, and S. Yen, Phys. Rev. C **44**, 93 (1991).

[13] M. Morlet, A. Willis, J. Van de Wiele, N. Marty, J. Guillot, H. Langevin-Joliot, L. Bimbot, L. Rosier, E. Tomasi-Gustafsson, G. W. R. Edwards, R. W. Fergerson, C. Glashausser, D. Beatty, A. Green, C. Djalali, F. T. Baker, and J. C. Duchazeaubeneix, Phys. Lett. B **247**, 228 (1990).

[14] C. Glashausser, K. W. Jones, F. T. Baker, L. Bimbot, H. Esbensen, R. W. Fergerson, A. Green, S. Nanda, and R. D. Smith, Phys. Rev. Lett. **58**, 2404 (1987).

[15] M. Morlet, F. T. Baker, D. Beatty, L. Bimbot, C. Djalali, G. W. R. Edwards, R. W. Fergerson, C. Glashausser, A. Green, J. Guillot, B. N. Johnson, F. Jourdan, H. Langevin-Joliot, N. Marty, L. Rosier, E. Tomasi-Gustafsson, J. Van de Wiele, A. Willis, and M. Y. Youn, in *Proceedings of the International Conference on Nuclear Reaction Mechanisms*, edited by E. Gadioli (Universita degli Studi di Milano, Varenna, Italy, 1991), p. 654.

[16] S. J. Seestrom-Morris, J. M. Moss, J. B. McClelland, W. D. Cornelius, T. A. Carey, N. M. Hintz, M. Gazzaly, M. A. Franey, S. Nanda, and B. Aas, Phys. Rev. C **26**, 2132 (1982).

[17] *Proceedings of the Third International Symposium on Polarization phenomena in nuclear reactions* (Univ. of Wisconsin Press, Madison, 1971).

[18] G. G. Ohlsen, Rep. Prog. Phys. **35**, 717 (1972).

[19] M. Morlet, T. Mandon, B. Bonin, C. Djalali, J. Van de Wiele, and A. Willis, in [15], p. 41.

[20] R. A. Arndt, L. D. Roper, R. A. Bryan, R. B. Clark, B. J. VerWest, and P. Signell, Phys. Rev. D **28**, 97 (1983).

[21] R. M. Haybron, Phys. Rev. **160**, 756 (1967).

[22] M. Lacombe, B. Loiseau, J. M. Richard, R. Vinh Mau, J. Côté, P. Pirès, and R. de Toureil, Phys. Rev. C **21**, 861 (1979).

[23] R. Beurtey, *Summer School, Nuclear and Particle Physics at Intermediate Energies*, Brentwood College School, British Columbia, Canada, 1975 (unpublished); J. Saudinos, J. C. Duchazeaubeneix, C. Laspalles, and R. Chaminade, Nucl. Instrum. Methods **11**, 77 (1973).

[24] B. Bonin, A. Boudard, H. Fanet, R. W. Fergerson, M. Garçon, C. Giorgetti, J. Habault, J. Le Meur, R. M. Lombard, J. C. Lugol, B. Mayer, J. P. Mouly, E. Tomasi-Gustafsson, J. C. Duchazeaubeneix, J. Yonnet, M. Morlet, J. Van de Wiele, A. Willis, G. Greeniaus,

G. Gaillard, P. Markowitz, C. F. Perdrisat, R. Abegg, and D. A. Hutcheon, Nucl. Instrum. Methods **A288**, 379 (1990).

[25] B. Bonin, A. Boudard, H. Fanet, R. W. Fergerson, M. Garçon, C. Giorgetti, J. Habault, J. Le Meur, R. M. Lombard, J. C. Lugol, B. Mayer, J. P. Mouly, E. Tomasi-Gustafsson, J. C. Duchazeaubeneix, J. Yonnet, M. Morlet, J. Van de Wiele, A. Willis, G. Greeniaus, G. Gaillard, P. Markowitz, C. F. Perdrisat, R. Abegg, and D. A. Hutcheon, Nucl. Instrum. Methods **A288**, 389 (1990).

[26] Commisariat à l'Energie Atomique Internal Report DPhN/Saclay No. 2526 (1989); Laboratoire National Saturne Internal Report LNS/Ph/91-32 (1991).

[27] J. Arvieux, S. D. Baker, A. Boudard, J. Cameron, T. Hasegawa, D. A. Hutcheon, C. Kerboul, G. Gaillard, and Nguyen Van Sen, Nucl. Instrum. Methods **A273**, 48 (1988).

[28] E. Tomasi-Gustafsson, J. Arvieux, Y. Bedfer, G. Milleret, J. Yonnet, P. Zupranski, A. Boudard, M. Garçon, L. Bimbot, B. N. J. Johnson, N. Marty, M. Morlet, L. Rosier, and A. Willis, Laboratoire National Saturne Internal Report LNS/Ph/91-27 (1991).

[29] H. Quechon, Ph.D. thesis, Université Paris XI, Orsay, 1980.

[30] R. W. Fergerson, Ph.D. thesis, University of Texas, Austin (1985) (Los Alamos National Laboratory Report No. LA-10554-T).

[31] S. Cohen and D. Kurath, Nucl. Phys. **73**, 1(1965); K. W. Jones, Ph.D. thesis, Rutgers University (1984) (Los Alamos Laboratory National Laboratory Report No. LA-10064-T).

[32] B. A. Brown, private communication.

[33] W. Unkelbach and J. Wambach, private communication.

[34] L. Bimbot, R. W. Fergerson, C. Glashausser, K. W. Jones, F. T. Baker, D. Beatty, V. Cupps, A. Green, and S. Nanda, Phys. Rev. C **42**, 2367 (1990).

[35] L. B. Rees, J. M. Moss, T. A. Carey, K. W. Jones, J. B. McClelland, and N. Tanaka, Phys. Rev. C **34**, 627 (1986).

[36] H. Toki, G. F. Bertsch, and D. Cha, Phys. Rev. C **28**, 1398 (1983).

[37] B. Castel, A. G. M. Hees, and L. Zamick, Nucl. Phys. **A415**, 30 (1984); T. S. Dumitrescu and T. Suzuki, *ibid.* **A423**, 277 (1984); B. Castel and A. G. Van Hees, Z. Phys. A **321**, 451 (1985).

[38] F. T. Baker, L. Bimbot, B. Castel, R. W. Fergerson, C. Glashausser, A. Green, O. Häusser, K. Hicks, K. W. Jones, C. A. Miller, S. K. Nanda, R. D. Smith, M. C. Vetterli, J. Wambach, R. Abegg, D. Beatty, V. Cupps, C. Djalali, R. Henderson, K. P. Jackson, R. G. Jeppesen, J. Lissantti, M. Morlet, R. S. Sawafta, W. Unkelbach, A. Willis, and S. Yen, Phys. Lett. B **237**, 337 (1990).

[39] A. Green and W. Unkelbach *et al.*, private communication.